

Figure 23. Asymmetric notched three-point bending test. Crack topology of the viscous three-field formulation (63) for (a) 58 000 elements and $\eta=2.5 \times 10^{-5}$ kNs/mm²; (b) 58 000 elements and $\eta=1.0 \times 10^{-6}$ kNs/mm²; (c) 79 000 elements and $\eta=2.5 \times 10^{-5}$ kNs/mm²; (d) crack trajectories obtained by Miehe and Güreses [20]; and (e) experimental crack patterns by Bittencourt *et al.* [28].

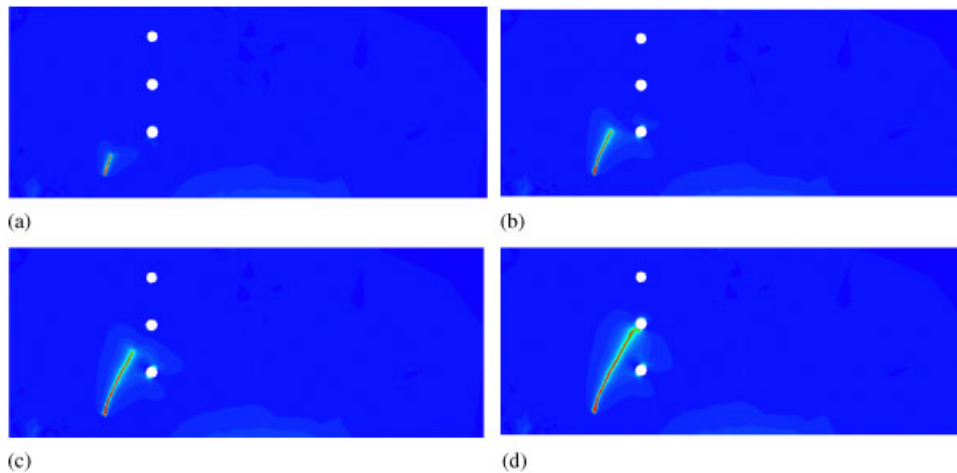


Figure 24. Asymmetric notched three-point bending test. Crack topology (a)–(d) for a mesh with 79 000 elements and a length-scale parameter $l=0.01$ mm.

formulation (63). The viscosity parameter is set to $\eta=5 \times 10^{-5}$ kN/mm². Figure 25(b) visualizes the crack in its final position in the undeformed configuration. Here, the crack is characterized by the iso-surface of the damage field for the fully damaged state $d(x)=1$. Figures 26(a)–(d)) depict the evolution of the phase-field at different stages of the deformation. As expected, the crack starts at the notch tip and propagates straight through the specimen. Figure 25(c) shows the final crack topology obtained by the configurational-force-driven sharp crack model. Here, crack propagation is based on the adaptive reorientation of critical segments and subsequent node doubling, see Güreses and Miehe [19]. In this scenario, the specimen is discretized with only 3738 linear tetrahedra. The crack shows some roughness but is almost planar. The final crack surfaces of both models are in very good agreement. The main drawback of the phase-field model lies